AIAA JOURNAL
Vol. 47, No. 7, July 2009

Effect of Stacking Sequence on Open-Hole Tensile Strength of Composite Laminates

Stephen R. Hallett*
University of Bristol, Bristol, England BS8 1TR, United Kingdom
Wen-Guang Jiang†
Yanshan University, 066004 Qinhuangdao, People's Republic of China
and
Michael R. Wisnom‡
University of Bristol, Bristol, England BS8 1TR, United Kingdom

DOI: 10.2514/1.41244

The effect of a ply stacking sequence on the open-hole tensile strength of composite laminates has been investigated both numerically and experimentally. A finite element technique has been developed that includes the subcritical damage within and between the plies. It is thus able to capture, in some detail, the effects of variation in stacking sequence. All possible permutations of 0, 90, and ±45 deg plies in a quasi-isotropic layup have been analyzed. Variations in strength have been observed and explained in terms of subcritical damage development. Two stacking sequences showing different behavior were chosen for scaling in the thickness direction by increasing the ply thickness. Analysis of the first predicted a significant decrease in strength and a change in failure mode from fiber-dominated to delamination-dominated failure with increasing thickness. The second predicted no such decrease in strength or change of failure mode. Both of these stacking sequences were then tested experimentally at both thicknesses, and excellent agreement with the numerical models was obtained, both in terms of damage mode and failure stress.

Nomenclature

E_{11}	=	fiber direction modulus
E_{22}	=	transverse modulus (in plane)
E_{33}	=	transverse modulus (out of plane)
G_{12}	=	12-direction shear modulus
G_{13}	=	13-direction shear modulus
G_{23}	=	23-direction shear modulus
G_I	=	mode I energy release rate
G_{II}	=	mode II energy release rate
G_{IC}	=	mode I critical energy release rate
G_{IIC}	=	mode II critical energy release rate
m	=	Weibull modulus
P	=	probability of survival
V	=	volume
V_i	=	volume of the ith element
α	=	fracture criterion mixed-mode index
α_{11}	=	fiber direction coefficient of thermal expansion
α_{22}	=	transverse coefficient of thermal expansion (in plane)
α_{33}	=	transverse coefficient of thermal expansion (out of plane)
ν_{12}	=	12-direction Poisson's ratio
ν_{13}	=	13-direction Poisson's ratio
ν_{23}	=	23-direction Poisson's ratio
σ	=	applied stress
σ_i	=	stress in the ith element
σ_{unit}	=	unidirectional failure stress of a unit volume
σ_0	=	characteristic strength
σ_{I}	=	normal interlaminar tensile stress
σ_{II}	=	shear stress resultant
$\sigma_{\text{I}}^{\max}$	=	interlaminar tensile strength
$\sigma_{\text{II}}^{\max}$	=	interlaminar shear strength

Presented as Paper 2334 at the 48th AIAA/ASME/ASCE/AHS/ASC Structures, Structural Dynamics, and Materials Conference, Honolulu, HI, 23–26 April 2007; received 26 September 2008; revision received 6 March 2009; accepted for publication 23 March 2009.

*Senior Lecturer in Aerospace Structures, Department of Aerospace Engineering, Advanced Composites Centre for Innovation and Science.
†Professor, School of Mechanical Engineering.
‡Professor, Aerospace Structures, Department of Aerospace Engineering, Advanced Composites Centre for Innovation and Science.

I. Introduction

THE scaling effect on the strength of composites is a well-documented phenomenon [1] that generally shows a decrease in strength with increasing specimen size. Similarly, the effect of scale on notched strength has been widely researched [2–4]. A comprehensive experimental program by Green et al. [4] on open-hole tension tests investigated a wide range of specimen sizes. It was noted that damage occurred in most specimens at load levels somewhat below the ultimate failure stress and that this subcritical damage strongly affected the results. For different specimen sizes and different thickness scaling routines (ply level or sublaminate level), different failure mechanisms were observed. These were classified into three categories: brittle, pullout, and delamination (Fig. 1). The first showed a clean break across the width of the specimen at the hole, with every ply failing by fiber failure. The second showed a more distributed damage, with some of the 45 deg plies failing by matrix cracking and delamination and hence pulling out from between the adjacent plies with the 0 deg plies and some of the 45 deg plies still failing by fiber failure. The third mechanism showed gross delamination that started at the hole and propagated back to the gripping regions. This was sudden and catastrophic and caused a significant drop on the load-displacement curve. The 0 deg plies generally remained intact during this process and thus could continue to carry some residual load, but for all practical purposes, the specimen had lost its structural integrity and was thus considered to have failed. A change in specimen size can cause a change in failure mode, which in turn can have a significant effect on strength results. These different failure modes are not generally taken into account in studies on scaling and size effect. A notable observation from these tests was the development of subcritical damage, which

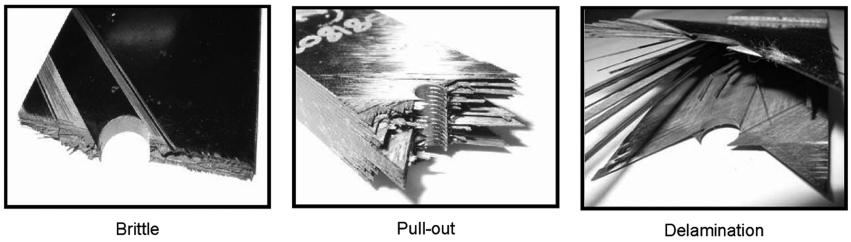

Fig. 1 Failure mechanisms observed in open-hole tensile tests [4].

started as matrix cracks accompanied by small areas of delamination at the hole edge predominantly at the surface 45/90 deg interface. Once these delaminations progressed, they were able to join up with delaminations at the free edge and then drop down through the thickness of the laminate via interconnecting matrix cracks. This process was only halted once a 0 deg ply was encountered through which the delamination could not pass or when the fiber failure strain was reached.

From this dependence of ultimate strength on the progression sequence of subcritical damage, it might well be expected that the stacking sequence of a laminate would affect results. This phenomenon has been investigated by a number of authors. Lagace [5] looked at $[\pm\theta/0]$, $[0/\pm\theta]$, and $[+\theta/0/-\theta]$ laminates, with θ equal to 15, 30, 45, 60, 75, and 90 deg for circular holes with 3.175, 6.35, 9.525, and 12.7 mm diameters. It was observed that the failure stresses of the $[+\theta/0/-\theta]$ laminates differed significantly from those of the $[\pm\theta/0]$ and $[0/\pm\theta]$ laminates, which had the 0 deg plies on the surface or centerline and generally had the same strength for a given fiber angle and hole diameter. For laminates with θ less than 45 deg, the first class of laminates was stronger, and for θ greater than 45 deg, they were weaker, with θ equal to 45 deg, giving approximately uniform strengths. These differences were attributed to interlaminar stresses causing delaminations and constraining effects from neighboring plies, which are different for each laminate. Walsh and Ochoa [6] examined a range of quasi-isotropic laminates with multiple holes (circular and square) at two diameters: 6.35 and 9.5 mm. Four stacking sequences were tested: $[0/45/-45/90]_{2S}$, $[45/-45/0/90]_{2S}$, $[45/0/-45/90]_{2S}$, and $[90/-45/45/0]_{2S}$. The description of the failed specimens is similar to that previously described as a pullout-type failure. Laminates with 0 deg plies on the centerline or surface were consistently stronger than those with 45 or 90 deg plies on the surface. A similar result of higher strengths for quasi-isotropic laminates with surface 0 deg plies is also reported by Jen et al. [7]. Their discussion and explanation for these differences also centers on variations in interlaminar stress, which in turn drives the formation of delaminations. These considerations of the effect of stacking sequence have not generally taken into account the influence of intraply splitting, which has been carefully observed in cross-ply laminates by Kortschot and Beaumont [8] and by Hallett and Wisnom [9] for quasi-isotropic laminates. This is known to be significant: first, for the blunting effect it has on the notched stress concentration, and second, for the way in which it allows delaminations to form, join up, and propagate through the laminate [10].

Here, an analysis technique is presented that explicitly takes account of the intraply splits and their interaction with interply delamination. The two competing ultimate failure modes of in-plane fiber failure and delamination, driven by out-of-plane stresses, are predicted and compared. These different failure mechanisms are particularly significant when either specimen size or stacking sequence is varied, as they can both have a significant effect on laminate notched strength. In the study on scaled open-hole tensile strength in [4], only one stacking sequence was used for all tests. Here, all possible stacking sequences are investigated numerically and two of particular interest are selected for thickness scaling by the ply blocking method and are experimentally validated.

II. Modeling Technique

A finite element technique has been developed to predict the failure of notched composite laminates made from unidirectional prepreg [11] and successfully used to predict the observed scaling effect [12]. It was found necessary to include the subcritical damage that occurs both within each ply and between each ply to fully capture the stress field as it changes with increasing damage levels before ultimate failure. This has been done by inserting interface elements (based on a cohesive zone model) into the model at critical locations. Because each ply is modeled explicitly, it can be expected that in addition to capturing the global behavior, it is also capable of predicting differences that occur as a result of variations in stacking sequence.

A. Intralaminar Splitting and Interlaminar Delamination

The interface element used to model the splitting and delamination is effectively a nonlinear spring inserted between two initially

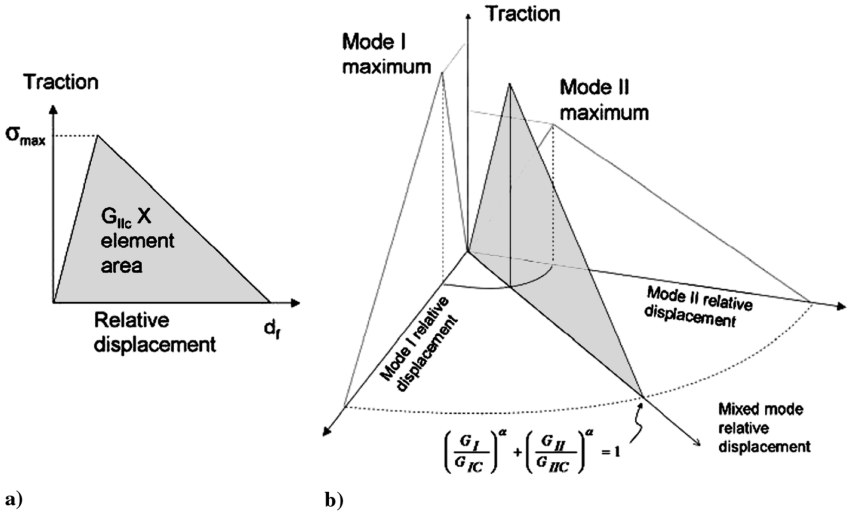

Fig. 2 Traction-relative displacement for interface element a) single mode and b) mixed mode.

coincident nodes. The formulation used here has a bilinear traction-displacement law, as shown in Fig. 2. This is initially linear elastic up to the maximum stress, after which a linear softening law is applied to reduce the stress such that the area under the curve is equal to the critical fracture energy. This behavior requires a damage initiation criterion and a complete failure criterion, both of which must be applicable to mixed-mode loading scenarios. The following simple quadratic damage initiation criterion under a multi-axial stress state [Eq. (1)] has been successfully used to predict the onset of delamination in previous investigations [13,14] and is adopted here:

$$\sqrt{\left(\frac{\max(\sigma_I, 0)}{\sigma_I^{\max}}\right)^2 + \left(\frac{\sigma_{II}}{\sigma_{II}^{\max}}\right)^2} = 1 \tag{1}$$

where σ_I is the normal interlaminar tensile stress, σ_{II} is the shear stress resultant of the interface, $\sigma_I^{\max}$ is the interlaminar tensile strength, and $\sigma_{II}^{\max}$ is the interlaminar shear strength. It is assumed that any normal interlaminar compressive stress does not affect the onset of mode II delamination. The damage initiation locus represented by the relative nodal displacement corresponding to the softening onset can be determined by this expression.

Experimental results indicate that a significant number of interface failures under mixed-mode conditions can be covered by a power law [15–18] relating the mode I and mode II components. For complete failure of the interface element, Eq. (2) is thus adopted in the current formulation:

$$\left(\frac{G_I}{G_{IC}}\right)^{\alpha} + \left(\frac{G_{II}}{G_{IIc}}\right)^{\alpha} = 1 \tag{2}$$

where $\alpha \in (1.0 \sim 2.0)$ is an empirical parameter derived from mixed-mode tests; G_I and G_{II} are the energy release rates for pure mode I (opening) and pure mode II (shear), respectively; and G_{IC} and G_{IIC} are the critical energy release rates. The fully debonded locus represented by the relative displacement corresponding to the complete interface failure can be determined by this condition.

B. Fiber Failure Prediction

The preceding interface element behavior is sufficient to capture the splitting and delamination failure modes but does not predict fiber failure, which is the dominant failure mode in the case of the sublaminate-level scaled samples: for this, a separate criterion is required. The decrease in strength with increasing specimen size for a brittlelike material can be well explained using Weibull volumetric statistical strength theory. This has been extensively applied to fiber-dominated failures in composite materials [19–21]. This theory supposes that the strength of a brittlelike material is controlled by flaws that are statistically distributed. The simple two-parameter model states that the probability of survival P of a specimen subjected to a stress field σ over a volume V can be represented by Eq. (3):

$$P(\sigma) = \exp\left(-\int_V \left(\frac{\sigma}{\sigma_0}\right)^m \mathrm{d}V\right) \tag{3}$$

where σ_0 is the characteristic strength and m is the Weibull modulus.

Based on the assumption that two specimens of different size will have equal probability of survival at their respective failure loads, we can set up Eq. (4):

$$P(\sigma) = \exp\left(-\int_{V_1} \left(\frac{\sigma_1}{\sigma_0}\right)^m \mathrm{d}V\right) = \exp\left(-\int_{V_2} \left(\frac{\sigma_2}{\sigma_0}\right)^m \mathrm{d}V\right) \tag{4}$$

If the stress σ_2 on the right-hand side pertains to a unit volume of material V_2 with constant stress σ_{unit}, then Eq. (4) simplifies to

$$\int_V \left(\frac{\sigma}{\sigma_{\text{unit}}}\right)^m \mathrm{d}V = 1 \tag{5}$$

This allows comparison of any given stress state σ to a reference stress state to obtain a failure criterion. Using results from scaled unidirectional tensile tests [22] and a least-squares fit of $\ln \sigma$ vs $\ln V$, we can derive the equivalent material constants as $m = 41$ and $\sigma_{\text{unit}} = 3131$ MPa for 1 mm^3 of the IM7/8552 material used in this study. In cases in which delamination does not occur first, the Weibull criterion can be applied to predict overall specimen strength. To keep the numerical model simple, instead of incorporating the fiber failure algorithm directly into the finite element model, a sequential checking of the Weibull failure criterion throughout the loading history has been performed by postprocessing the stress results from the models containing interface elements used to predict delamination. The integration in the failure criterion becomes a summation over the elements in the finite element model:

$$\int_V \left(\frac{\sigma}{\sigma_{\text{unit}}}\right)^m \mathrm{d}V = \sum_{i=1}^{\text{total no. of solid elements}} \left(\frac{\sigma_i}{\sigma_{\text{unit}}}\right)^m V_i \geq 1 \tag{6}$$

where σ_i and V_i are the stress and volume of each element in turn. The critical failure load can be estimated to be the loading point at which the criterion is first met.

C. Model Setup

Finite element models of the open-hole specimens were created in the explicit code LS-Dyna to predict the failure of the tensile tests. Fully integrated solid elements were used with one element through the thickness of each ply block, which has been shown to be sufficient to achieve a converged solution [12]. A half-model through the thickness was used because the layups under investigation were all symmetric about the centerline. Thermal residual stresses were included in the model by applying a −160°C temperature reduction before mechanical loading to simulate cooldown from the 180°C processing temperature to a room temperature of 20°C. Mechanical loading was applied using a prescribed displacement on the nodes at the end of the gauge section at a rate sufficiently slowly so as not to induce dynamic effects. Interface elements were inserted between coincident nodes to predict the initiation and propagation of subcritical damage. For the intraply splitting interface elements were inserted within each ply, in a line tangential to the hole, in the fiber direction. In the 90 deg ply, an additional crack was inserted at the position of the maximum stress concentration. Experimental observations have indicated that these are the locations of the major splits that are significant to the overall specimen failure [23]. Inserting these lines within the mesh resulted in small degenerated elements around the hole that were removed, resulting in an octagonal-shaped hole. Although this will affect the linear elastic stress concentration, once the splitting initiates (as it does in all cases examined here), the stress concentration is relieved and the exact geometry of the hole does not affect results. For the interply delamination, interface elements were inserted between each ply block. This is shown schematically in Fig. 3.

D. Determination of Failure Mode

The failure mode of a given test configuration can be predicted using the preceding analysis techniques. In a simulated tensile test, loaded through applied displacement, subcritical damage in the form of local splitting and delamination will occur at the hole and free edge. Once this has progressed beyond a critical point, sudden and catastrophic delamination occurs, starting at the hole and propagating all the way back to the gripping region. This sudden delamination causes a significant drop on the load-displacement curve, both numerically (Fig. 4) and experimentally.

Because there is no fiber failure model embedded directly in the finite element algorithm, all laminates will eventually reach this point of catastrophic delamination, provided that a sufficiently large displacement is applied. However, during the physical damage development in experiments, there is a point at which the fiber failure stress is exceeded and the specimen fails. The relative stress levels at which this occurs compared with the damage development is a controlling factor to determine the failure modes observed in Fig. 1. The point of fiber failure in the analysis can be predicted using the

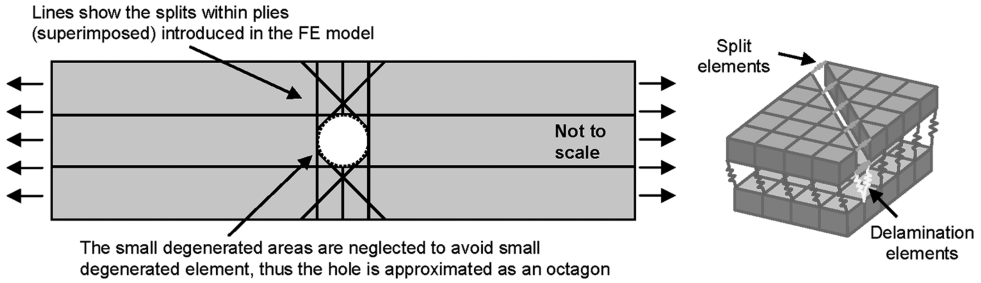

Fig. 3 Location of potential splits in which interface elements have been inserted and manner of insertion (FE denotes finite element).

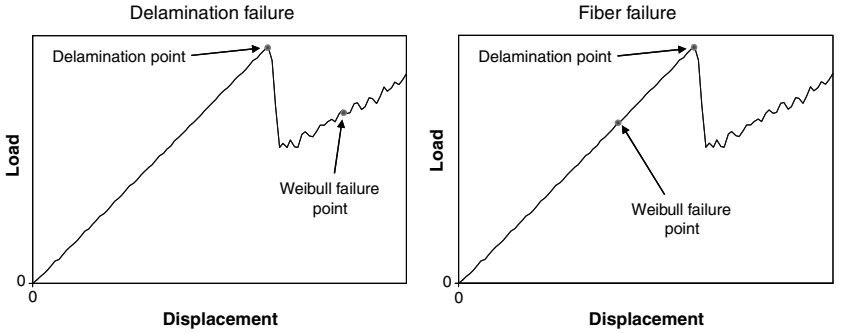

Fig. 4 Determination of the failure mode from the load/displacement curves.

Weibull statistical criterion and postprocessing method described previously. All analyses conducted were subject to this postprocessing routine and a Weibull failure point was determined. In some cases, this point occurred after the significant load drop caused by delamination, and in other cases, it occurred before. The first case, shown on the left of Fig. 4, can therefore be classified as a delamination failure, and the second case (Fig. 4, right) was classified as a fiber-dominated failure (brittle or pullout, as per Fig. 1). The analysis could not distinguish between the brittle and pullout-type failures, because both are due to fiber failure. Note that in all analyses, both a delamination point and a Weibull failure point could be determined.

III. Predicting the Effect of Stacking Sequence

A. Baseline Analyses

Each of the 12 possible stacking sequences of a 0, 90, ± 45 deg quasi-isotropic laminate has been analyzed using the preceding technique. The specimen geometry is given in Fig. 5. The material was IM7/8552 carbon/epoxy prepreg with 0.125 mm nominal ply thickness. The material properties used for both the interface elements [18] and the plies [24] are shown in Table 1.

For each layup, both a fiber failure stress (Weibull-based) and a delamination failure stress was obtained, shown in Fig. 6. The two stacking sequences in each of the subgroups a–f are the inverse of each other. In each case, the Weibull failure criterion was met before significant delamination occurred. They can all therefore be classed as fiber-dominated failures (brittle or pullout).

It was observed that the laminates could be divided into two groups based on their predicted fiber failure stress: those with the 0 deg plies at the surface or on the centerline (which have an average failure stress of approximately 600 MPa) and the rest (which had an average failure stress of approximately 500 MPa). Even though in all cases ultimate failure was predicted to occur by fiber rupture, there was still a certain amount of subcritical damage local to the hole. This affects the stress in the load bearing 0 deg plies and causes variations in the predicted fiber failure stress. Looking only at the intraply splitting damage at the point of predicted fiber failure in Fig. 7, the difference between the two groups is quite noticeable. Those with the 0 deg plies at the surface or on the centerline have a higher degree of splitting in the 0 deg plies than the second group, for which no discernible 0 deg splitting can be detected. The reduced constraint of the 0 deg plies on the surface or the thicker ply blocks of the 0 deg on the centerline causes the splitting to be greater in the first group. This splitting causes an effective blunting of the notch by relieving the stress concentration in the load bearing 0 deg plies local to the hole and thus allows a higher failure stress to be achieved. The effect of the 0 deg splitting on the stress state will in fact be greater than the lengths shown by the fully failed elements in Fig. 7. Ahead of the fully failed elements there will be a softening zone of elements between full failure and damage initiation, which can be as long as 4 mm for mode II [25] (i.e., greater than one hole diameter).

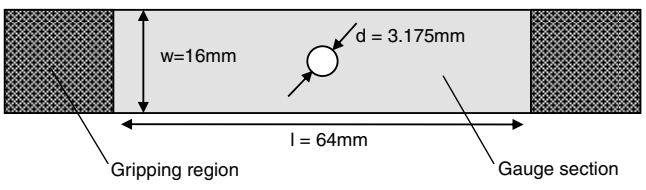

Fig. 5 Specimen dimensions.

B. Thickness Scaling

Two stacking sequences that were of particular interest (highlighted in Fig. 7) were chosen for further investigation. The first, $[-45/45/90/0]_s$, shows the smallest difference between

Table 1 Material properties used in analyses

Properties	Values
G_{IC}	0.2 N/mm
G_{IIC}	1.0 N/mm
α	1.0
$\sigma_I^{\max}$	60 MPa
$\sigma_{II}^{\max}$	90 MPa
E_{11}	161 GPa
$E_{22} = E_{33}$	11.38 GPa
$G_{12} = G_{13}$	5.17 GPa
G_{23}	3.98 GPa
$\nu_{12} = \nu_{13}$	0.32
ν_{23}	0.436
α_{11}	$0.0°C^{-1}$
$\alpha_{22} = \alpha_{33}$	$3 \times 10^{-5}°C^{-1}$

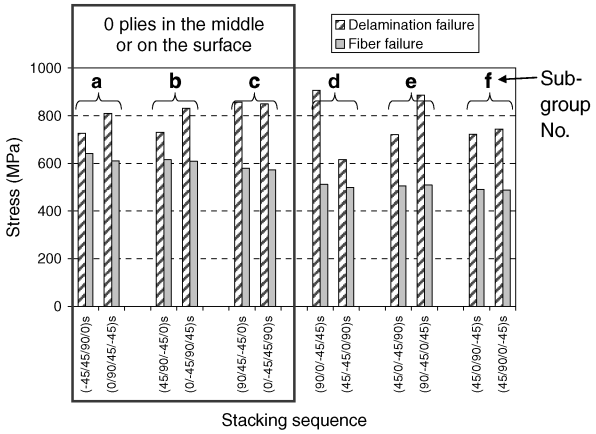

Fig. 6 Fiber and delamination stress for all permutations of 0, 90, ±45 deg stacking sequences.

predicted fiber failure and delamination stress, and the second, $[90/-45/0/45]_s$, shows one of the largest differences. When the thickness of a ply is increased (for example, by blocking two layers of prepreg together), the amount of energy available to propagate a delamination is doubled. The delamination area, however, is not increased, and thus the stress at which a delamination will propagate is lower in the thicker specimens [4]. This scaling effect was expected to have a significantly different influence on the two cases highlighted, due to the relative difference in fiber failure and delamination stress levels. Models of specimens 2 mm thick with two plies blocked together in each direction were therefore created to investigate the changes in strength and failure mode. This gave layups of $[45_2/-45_2/90_2/0_2]_s$ and $[90_2/-45_2/0_2/45_2]_s$, respectively.

In each case, a Weibull-based fiber failure stress and delamination stress was obtained from the analysis. Note the significant change in the relative positions of the delamination stress and Weibull failure stress on the stress-extension curves; these are shown in Fig. 8. The first layup, $[-45/45/90/0]_s$, was the strongest at 1 mm and had the

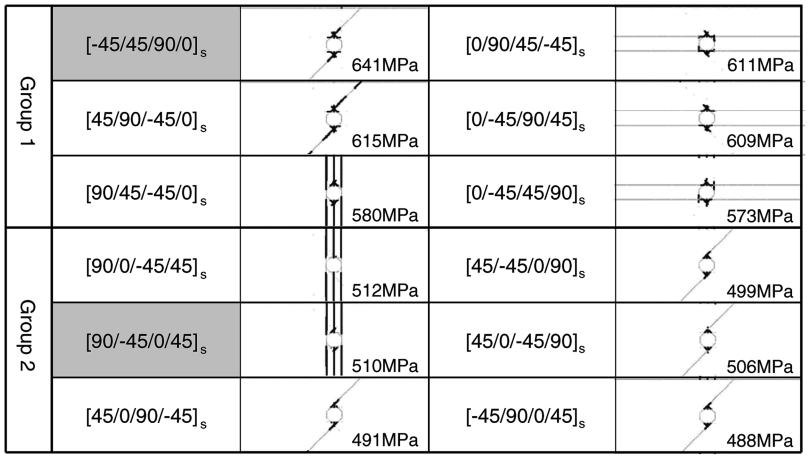

Fig. 7 Splitting damage at predicted failure load for all 12 stacking sequences.

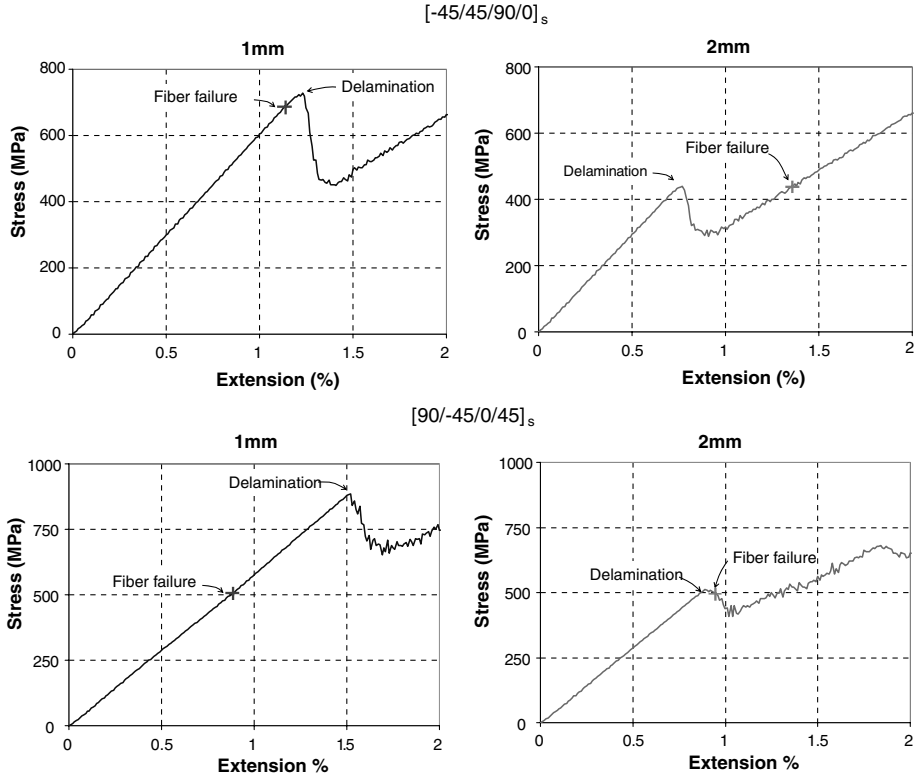

Fig. 8 Stress-extension plots for the two layups modeled at 1 and 2 mm thicknesses.

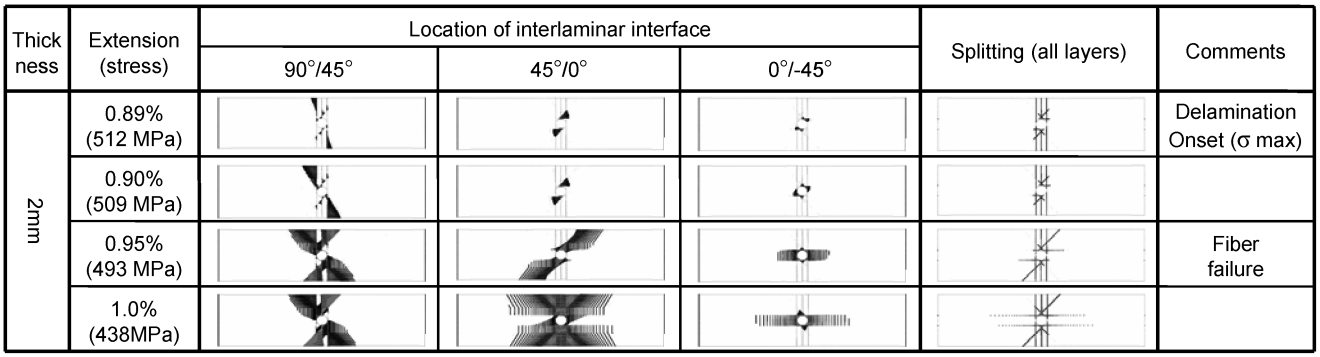

Fig. 9 Damage development sequence for 2-mm-thick $[90_2/-45_2/0_2/45_2]_s$ stacking sequence.

smallest difference between predicted fiber failure and delamination stress. When the ply block thickness is increased to 0.25 mm, 2 mm total laminate thickness, the delamination stress is significantly reduced. This reduction is sufficient to bring it below the point at which fiber failure was predicted to occur and therefore the predicted failure mode changes to delamination. The overall effect was to significantly reduce the laminate failure stress as thickness is increased from 1 to 2 mm: 442 MPa compared with 641 MPa.

The second layup, $[90/-45/0/45]_s$, was one of the weakest at 1 mm, due to the limited amount of 0 deg splitting and hence notch blunting, but had one of the largest differences between fiber failure and delamination stress. The increase in thickness to 2 mm again caused a reduction in predicted delamination stress. This reduction, however, did not bring the stress below that predicted by the Weibull criterion. In this case, the fiber failure prediction in fact occurs almost simultaneously to the delamination prediction, unlike the 1 mm case, in which there is a clear separation. Here, the load has reached a local maximum, and it is at this point that the Weibull criterion is exceeded, before any significant reduction in load due to the delamination. Figure 9 shows the sequence of damage growth. Each row shows a plan view of the specimen, with the predicted damage at an increasing applied extension. The stress is calculated from the nodal reaction forces. Predicted delamination at each of the three interfaces is shown separately. The dark colored areas indicate completely failed interface elements. In areas far away from the hole, this can appear as a series of lines or points instead of continuous color, due to the coarser mesh used in these areas. The predicted splitting in all plies is shown simultaneously in a single image at each load, on the right-hand side. It was felt that in this case, because the delamination had not extensively propagated, it should still be classed as a fiber failure. In practice, because the failure stresses are so close, only a small amount of delamination is likely to be necessary to cause a local stress concentration and trigger fiber failure.

IV. Experimental Validation

To validate the preceding analyses, specimens were manufactured from unidirectional carbon/epoxy prepreg (Hexply IM7/8552) with dimensions as per Fig. 5. Large flat plates were laid up and cured according to the manufacturers' recommended cure cycle. From these plates, the 16-mm-wide specimens were cut using a water-cooled diamond cutting wheel. The holes were initially drilled undersized and then reamed to the final 3.175 mm diameter. Glass/epoxy end tabs were bonded on to the specimens to prevent any damage from gripping in the test machines. The two stacking sequences identified and modeled in Sec. III.B were used. The nominal ply thickness was 0.125 mm, giving a baseline laminate thickness of 1 mm in each case. Each stacking sequence was then scaled in the thickness direction by doubling up the plies (ply-level scaling), giving stacking sequences of $[45_2/-45_2/90_2/0_2]_s$ and $[90_2/45_2/0_2/-45_2]_s$, with a nominal laminate thickness of 2 mm. For each layup, 8 specimens were tested in tension at a rate of 0.5 mm/min, and failure was defined as a load drop greater than 5%.

Both of the 1-mm-thick layups failed by fiber failure with some evidence of pullout of the off axis plies, as can be seen in Figs. 10a and 10b. The $[45/-45/90/0]_s$ laminate failed at an average stress of 563 MPa, and the $[90/45/0/-45]_s$ laminate failed at 481 MPa. This follows the same trend as predicted by the analysis, although the exact strength values show some difference to the predicted 627 and 506 MPa strengths, respectively. The 2-mm-thick specimens of the first stacking sequence, $[45_2/-45_2/90_2/0_2]_s$, showed a change in failure mode from the fiber-dominated failure in the 1-mm-thick specimens to delamination in the 2-mm-thick specimens. For this failure mode, there is significant delamination that starts at the hole and extends back to the grips, covering the entire gauge section (see Fig. 10c). This event causes a load drop greater than 5%. Although the 0 deg plies remain intact and can carry further tensile load, to all intents and purposes, the specimen has lost all structural integrity and is therefore deemed to have failed. The average failure load for these laminates was 474 MPa, significantly below that of the 1-mm-thick specimens. This matches well with the 442 MPa predicted by the analysis, which also captured the change in failure mode to delamination.

The second 2-mm-thick stacking sequence, $[90_2/45_2/0_2/-45_2]_s$, did not change failure mode with increased thickness. Instead, it presented a fiber-dominated failure pattern (Fig. 10d) very similar to the 1-mm-thick laminate for this same stacking sequence. This resulted in an average failure stress of 499 MPa, slightly higher than the thinner specimens and in very good agreement with the 512 MPa predicted by the analysis. It was noted during the tests that a large number of cracking sounds could be heard before final failure that were not present in the 1-mm-thick tests. This gives further credibility to the analysis result, which showed there to be significant

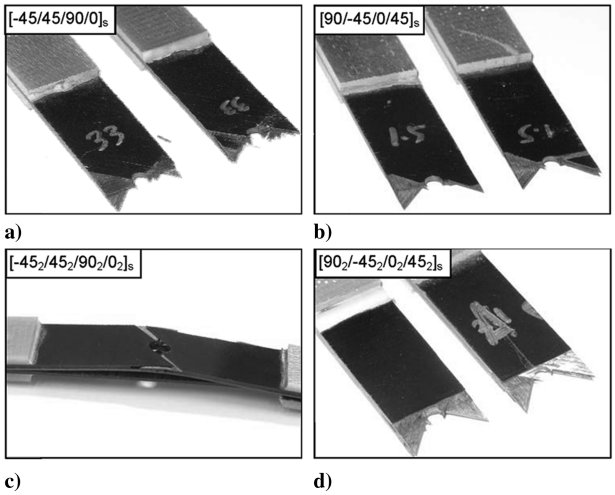

Fig. 10 Photographs of failed specimens a) $[-45/45/90/0]_s$, b) $[90/-45/0/45]_s$ showing fiber failure, c) $[45_2/-45_2/90_2/0_2]_s$ showing delamination failure, and d) $[90_2/-45_2/0_2/45_2]_s$ showing fiber failure.

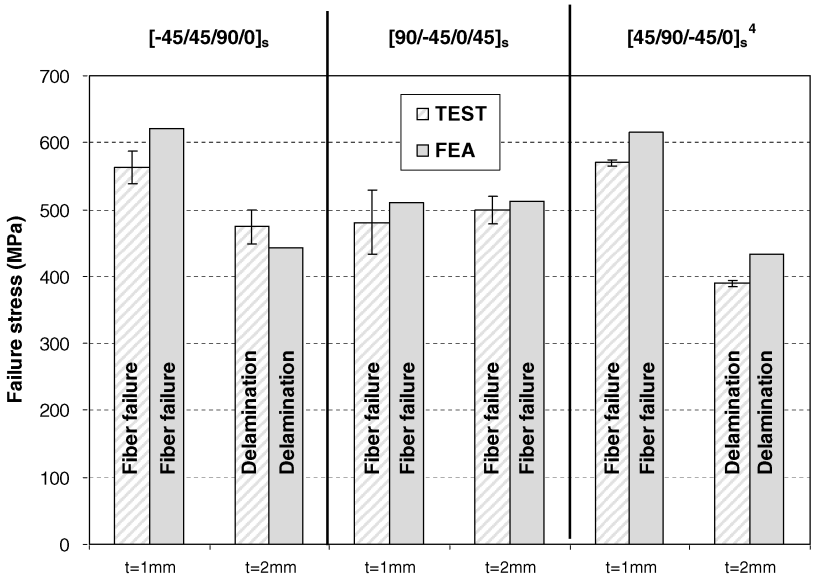

Fig. 11 Test to analysis comparison.

localized matrix cracking and delamination before final fiber failure. The strength of this laminate at 1 mm thick was significantly below that of the $[45/-45/90/0]_s$ stacking sequence. At 2 mm thick, it showed no strength reduction due to thickness scaling and in fact was stronger than the $[45_2/-45_2/90_2/0_2]_s$ stacking sequence. The experimental and numerical results are summarized graphically in Fig. 11, together with those of the previous stacking sequence investigated in [4]. The failure modes and strength variation for this third stacking sequence, $[45/90/-45/0]_s$, follow that of the first, $[45/-45/90/0]_s$, with only minor variation. This is due to the similarity of the layup in having the 0 deg ply on the centerline. It can be seen that excellent correlation has been achieved for failure mode and strength prediction. In all cases, the correct trends have been captured by the models, and differences in absolute values are generally within typical experimental variation. Note that both of the ply thicknesses used here are those of commercially available prepreg systems, and the reported results do not involve excessive ply blocking.

V. Conclusions

A modeling technique has been developed that is able to capture the details of subcritical damage development at the level of individual plies in notched tensile specimens. This uses only independently measured input data and does not require any further fitting parameters. This has allowed a detailed study to be undertaken on the effect of variation of stacking sequence on open-hole tensile strength. It has been shown that for quasi-isotropic layups, there exist a range of failure modes and strengths that are strongly dependent on the stacking sequence of the individual plies. For all 12 possible permutations of a 0, 90, and ± 45 deg laminate, there is a 28% difference in strength predicted between the weakest and strongest configurations. This can be explained in terms of the subcritical damage that develops in the specimens before ultimate failure. If ply thickness is increased from 0.125 to 0.25 mm for the case of the $[45/-45/90/0]_s$ stacking sequence, there is a predicted change in failure mode accompanied by a significant decrease in strength. For the $[90/45/0/-45]_s$ stacking sequence, the prediction is for no change in failure mode and for the strength to remain approximately constant. These results have been verified by experimental investigation, and good correlation was obtained in terms of both failure mode and strength.

Acknowledgments

The authors gratefully acknowledge the support of the U.K. Engineering and Physical Sciences Research Council (grant no. GR/R89462), the U.K. Ministry of Defence, and Airbus U.K. as well as the supply of material by Hexcel Composites.

References

[1] Wisnom, M. R., "Size Effects in the Testing of Fiber-Composite Materials," *Composites Science and Technology*, Vol. 59, No. 13, 1999, pp. 1937–1957. doi:10.1016/S0266-3538(99)00053-6

[2] Awerbuch, J., and Madhukar, M. S., "Notched Strength of Composite Laminates: Predictions and Experiments—A Review," *Journal of Reinforced Plastics and Composites*, Vol. 4, No. 1, 1985, pp. 3–159. doi:10.1177/073168448500400102

[3] Camanho, P. P., Maimi, P., and Davila, C. G., "Prediction of Size Effects in Notched Laminates Using Continuum Damage Mechanics," *Composites Science and Technology*, Vol. 67, No. 13, 2007, pp. 2715–2727. doi:10.1016/j.compscitech.2007.02.005

[4] Green, B. G., Wisnom, M. R., and Hallett, S. R., "An Experimental Investigation into the Tensile Strength Scaling of Notched Composites," *Composites, Part A: Applied Science and Manufacturing*, Vol. 38, No. 3, 2007, pp. 867–878. doi:10.1016/j.compositesa.2006.07.008

[5] Lagace, P., "Notch Sensitivity and Stacking Sequence of Laminated Composites," *Composite Materials: Testing and Design (Seventh Conference)*, STP 893, edited by J. M. Whitney, ASTM International, Philadelphia, 1986, pp. 161–76.

[6] Walsh, T. J., and Ochoa, O. O., "Composites with Multiple Cutouts," *Composite Structures*, Vol. 24, No. 2, 1993, pp. 117–124. doi:10.1016/0263-8223(93)90033-M

[7] Jen, M. H. R., Kau, Y. S., and Hsu, J. M., "Initiation and Propagation of Delamination in a Centrally Notched Composite Laminate," *Journal of Composite Materials*, Vol. 27, No. 3, 1993, pp. 272–302. doi:10.1177/002199839302700303

[8] Kortschot, M. T., and Beaumont, P. W. R., "Damage Mechanics of Composite-Materials, 1: Measurements of Damage and Strength," *Composites Science and Technology*, Vol. 39, No. 4, 1990, pp. 289–301. doi:10.1016/0266-3538(90)90077-I

[9] Hallett, S. R., and Wisnom, M. R., "Experimental Investigation of Progressive Damage and the Effect of Layup in Notched Tensile Tests," *Journal of Composite Materials*, Vol. 40, No. 2, 2006, pp. 119–141. doi:10.1177/0021998305053504

[10] Hallett, S. R., Jiang, W. G., Khan, B., and Wisnom, M. R., "Modelling the Interaction Between Matrix Cracks and Delamination Damage in Scaled Quasi-Isotropic Specimens," *Composites Science and Technology*, Vol. 68, No. 1, 2008, pp. 80–89. doi:10.1016/j.compscitech.2007.05.038

[11] Hallett, S. R., and Wisnom, M. R., "Numerical Investigation of Progressive Damage and the Effect of Layup in Notched Tensile Tests," *Journal of Composite Materials*, Vol. 40, No. 14, 2006, pp. 1229–1245.

doi:10.1177/0021998305057432
[12] Jiang, W. G., Hallett, S. R., Green, B. G., and Wisnom, M. R., "A Concise Interface Constitutive Law for Analysis of Delamination and Splitting in Composite Materials and Its Application to Scaled Notched Tensile Specimens," *International Journal for Numerical Methods in Engineering*, Vol. 69, No. 9, 2007, pp. 1982–1995. doi:10.1002/nme.1842
[13] Brewer, J. C., and Lagace, P. A., "Quadratic Stress Criterion for Initiation of Delamination," *Journal of Composite Materials*, Vol. 22, No. 12, 1988, pp. 1141–1155. doi:10.1177/002199838802201205
[14] Cui, W. C., Wisnom, M. R., and Jones, M., "A Comparison of Failure Criteria to Predict Delamination of Unidirectional Glass Epoxy Specimens Waisted Through the Thickness," *Composites*, Vol. 23, No. 3, 1992, pp. 158–166. doi:10.1016/0010-4361(92)90436-X
[15] Borg, R., Nilsson, L., and Simonsson, K., "Simulation of Delamination in Fiber Composites with a Discrete Cohesive Failure Model," *Composites Science and Technology*, Vol. 61, No. 5, 2001, pp. 667–677. doi:10.1016/S0266-3538(00)00245-1
[16] Pinho, S. T., Iannucci, L., and Robinson, P., "Formulation and Implementation of Decohesion Elements in an Explicit Finite Element Code," *Composites, Part A: Applied Science and Manufacturing*, Vol. 37, No. 5, 2006, pp. 778–789. doi:10.1016/j.compositesa.2005.06.007
[17] Juntti, M., Asp, L. E., and Olsson, R., "Assessment of Evaluation Methods for the Mixed-Mode Bending Test," *Journal of Composites Technology and Research*, Vol. 21, No. 1, 1999, pp. 37–48. doi:10.1520/CTR10611J
[18] Jimenez, M. A., and Miravete, A., "Application of the Finite-Element Method to Predict the Onset of Delamination Growth," *Journal of Composite Materials*, Vol. 38, No. 15, 2004, pp. 1309–1335. doi:10.1177/0021998304042734
[19] Wisnom, M. R., "Relationship Between Strength Variability and Size Effect in Unidirectional Carbon-Fiber Epoxy," *Composites*, Vol. 22, No. 1, 1991, pp. 47–52. doi:10.1016/0010-4361(91)90102-M
[20] Wisnom, M. R., and Atkinson, J. W., "Reduction in Tensile and Flexural Strength of Unidirectional Glass Fiber-Epoxy with Increasing Specimen Size," *Composite Structures*, Vol. 38, Nos. 1–4, 1997, pp. 405–411. doi:10.1016/S0263-8223(97)00075-5
[21] Wisnom, M. R., "The Relationship Between Tensile and Flexural Strength of Unidirectional Composites," *Journal of Composite Materials*, Vol. 26, No. 8, 1992, pp. 1173–1180. doi:10.1177/002199839202600805
[22] Wisnom, M. R., Khan, B., and Hallett, S. R., "Size Effects in Unnotched Tensile Strength of Unidirectional and Quasi-Isotropic Carbon/Epoxy Composites," *Composite Structures*, Vol. 84, No. 1, 2008, pp. 21–28. doi:10.1016/j.compstruct.2007.06.002
[23] Hallett, S. R., "Predicting Progressive Delamination via Interface Elements," *Delamination Behaviour of Composites*, edited by S. Sridharan, Woodhead, Cambridge, England, U.K., 2008.
[24] O'Brien, T. K., and Krueger, R., "Analysis of Ninety Degree Flexure Tests for Characterization of Composite Transverse Tensile Strength," NASA TM-2001-211227, 2001.
[25] Harper, P. W., and Hallett, S. R., "Cohesive Zone Length in Numerical Simulations of Composite Delamination," *Engineering Fracture Mechanics*, Vol. 75, No. 16, 2008, pp. 4774–4792. doi:10.1016/j.engfracmech.2008.06.004

A. Roy
Associate Editor